DETECTION OF GAMMA RAYS OF UP TO 50 TeV FROM THE CRAB NEBULA

T. Tanimori[1], K. Sakurazawa[1], S. A. Dazeley[2], P.G. Edwards[2,3], T. Hara[4], Y. Hayami[1], S. Kamei[1], T. Kifune[5], T. Konishi[6], Y. Matsubara[7], T. Matsuoka[7], Y. Mizumoto[8], A. Masaike[9], M. Mori[5,10], H. Muraishi[11], Y. Muraki[7], T. Naito[12], S. Oda[6], S. Ogio[1], T. Osaki[1], J. R. Patterson[2], M. D. Roberts[2,5], G. P. Rowell[2,5], A. Suzuki[6], R. Suzuki[1], T. Sako[7], T. Tamura[13], G. J. Thornton[2,5], R. Susukita[9,14], S. Yanagita[11], T. Yoshida[11], and T. Yoshikoshi[1,5]

---

[1]Department of Physics, Tokyo Institute of Technology, Meguro-ku, Tokyo 152, Japan

[2]Department of Physics and Mathematical Physics, University of Adelaide, South Australia 5005, Australia

[3]Institute of Space and Astronautical Science, Sagamihara, Kanagawa 229, Japan

[4]Faculty of Management Information, Yamanashi Gakuin University, Kofu, Yamanashi 400, Japan

[5]Institute for Cosmic Ray Research, University of Tokyo, Tanashi, Tokyo 188, Japan

[6]Department of Physics, Kobe University, Kobe, Hyogo 637, Japan

[7]Solar-Terrestrial Environment Laboratory, Nagoya University, Nagoya, Aichi 464, Japan

[8]National Astronomical Observatory, Mitaka, Tokyo 181, Japan

[9]Department of Physics, Kyoto University, Kyoto, Kyoto 606-01, Japan

[10]Department of Physics, Miyagi University of Education, Sendai, Miyagi 980, Japan

[11]Faculty of Science, Ibaraki University, Mito, Ibaraki 310, Japan

[12]Department of Earth and Planetary Physics, University of Tokyo, Bunkyo-ku, Tokyo 113, Japan

[13]Faculty of Engineering, Kanagawa University, Yokohama, Kanagawa 221, Japan

[14]Institute of Physical and Chemical Research, Wako, Saitama 351-01, Japan

Received ______________________; accepted ______________________

to be submitted to Astrophysical Journal Letters

ABSTRACT

Gamma rays with energies greater than 7 TeV from the Crab pulsar/nebula have been observed at large zenith angles, using the Imaging Atmospheric Technique from Woomera, South Australia. CANGAROO data taken in 1992, 1993 and 1995 indicate that the energy spectrum extends up to at least 50 TeV, without a change of the index of the power law spectrum.

The observed differential spectrum is $(2.01 \pm 0.36) \times 10^{-13}(E/7\,\mathrm{TeV})^{-2.53 \pm 0.18}$ $\mathrm{TeV}^{-1}\mathrm{cm}^{-2}\mathrm{s}^{-1}$ between 7 TeV and 50 TeV. There is no apparent cut-off.

The spectrum for photon energies above $\sim$10 TeV allows the maximum particle acceleration energy to be inferred, and implies that this unpulsed emission does not originate near the light cylinder of the pulsar, but in the nebula where the magnetic field is not strong enough to allow pair creation from the TeV photons. The hard gamma-ray energy spectrum above 10 TeV also provides information about the varying role of seed photons for the inverse Compton process at these high energies, as well as a possible contribution of π°-gamma rays from proton collisions.

Subject headings: gamma rays:observations – nebulae:individual (Crab nebula)

1. Introduction

In the 50 MeV to 10 GeV energy range the Crab emits both pulsed emission, from the central neutron star, and unpulsed emission, from the surrounding nebula (Nolan et al. 1993). The Crab nebula has been extensively studied from radio and optical to X-ray bands, and these photons are believed to originate as synchrotron emission from high energy electrons accelerated up to $\sim$ 100 TeV in the nebula (De Jager & Harding 1992 hereafter JH92; Atoyan & Aharonian 1996 hereafter AA96). The higher energy component, above $\sim$1 GeV, however, is thought to be produced by inverse Compton (IC) scattering between these very high energy electrons and ambient photons in the nebula. In the wide range from GeV to hundreds of TeV, gamma rays are expected to emanate from the Crab nebula via the IC process. Spectra have been calculated for various theoretical scenarios based on the Synchrotron Self Compton (SSC) model, using the synchrotron spectrum obtained from observations of radio to MeV gamma rays as seed photons (JH92;AA96). The predicted spectra for synchrotron and IC emission are sensitive to conditions within the nebula such as the magnetic field, the nature of the seed photons, and the maximum energy of high energy electrons, which allow us to test these models. In particular, all models predict that the shape of the spectrum becomes more sensitive to a change of the parameters of the nebula as the gamma-ray energy increases.

Observations of the IC domain have been made in the 0.1–10 GeV region by *EGRET* (Nolan et al. 1993; De Jager et al. 1996) and the 0.2–10 TeV region by imaging air Čerenkov telescopes (IACTs) (Vacanti et al. 1991; Goret et al. 1993; Tanimori et al. 1994 hereafter T94; Djannati-Atai et al. 1995; Aharonian et al. 1997; Cater-Lewis et al. 1997). *EGRET* observations have revealed a break in the energy spectrum of the unpulsed component from the Crab nebula above 0.1 GeV, which is believed to signal the change from synchrotron radiation by several hundreds TeV electrons at lower energies to IC emission at higher

energies. Unpulsed emission above 200 GeV up to 10 TeV has been detected by several IACTs with high statistics, although there still remains considerable uncertainty in the absolute flux and the spectral index. However, there exists only one observation of the detection for gamma rays above $\sim$ 10 TeV with limited statistics: by the Themistocle group with a multiple small mirror system (Djannati-Atai et al. 1995).

As pointed out above, the observation of gamma rays in the energy range above 10 TeV is the key to understanding of the IC process in the nebula. The large zenith angle technique (Sommers & Elbert 1987) was used by the CANGAROO group in the detection of gamma rays from the Crab in 1992 to obtain a single integral flux point of $(7.6 \pm 1.9) \times 10^{-13}$ $\mathrm{cm^{-2}s^{-1}}$ above 7 TeV at large zenith angles, $\sim$53°(T94), and has provided the current best sensitivity for detecting >10 TeV gamma rays among the various methods.

2. Observation

The observations reported here were made with the 3.8m telescope of the CANGAROO collaboration (Patterson and Kifune 1992), which is located at Woomera in South Australia (136°47′E and 31°06′S). The high resolution camera, set at the prime focus, consists of small square-shaped photomultiplier tubes of 10mm $\times$ 10mm size (Hamamatsu R2248). The number of photomultipliers was 220 in 1993 and was increased to 256, in a 16$\times$16 square pattern, in 1995 giving a total field of view of about 3°. The details of the camera and telescope are given in Hara et al. (1993). After the observations in 1992, the Crab was observed again at zenith angles of 53°–56° in two seasons; from 1993 December to 1994 January, and from 1995 December to 1996 January. In order to monitor the cosmic ray background contained in 'on-source' data, 'off-source' runs were also done as described in T94. In order to obtain an energy spectrum, 1992 data was analyzed again with 1993 and 1995 data. The total observation times in those three years used in this analysis were

2.22×10^5 s (1.36×10^5 s for 1993 and 1995 data) for on-source data and 2.04×10^5 s (1.20×10^5 s for 1993 and 1995 data) for off source data.

3. Analysis and Result

The imaging analysis of the data is based on parameterization of the elongated shape of the Čerenkov light image as: “width”,“length”, “distance” (location), “conc” (shape), and the image orientation angle α (Hillas 1985; Weekes et al. 1989). We analyzed the data of 1992, 1993, and 1995 observations by the similar parameters used in T94; the gamma-ray selection criteria used here are $0^\circ\!.02 \leq$ length $\leq 0^\circ\!.33$, $0^\circ\!.06 \leq$ width $\leq 0^\circ\!.13$ and $0^\circ\!.3 \leq$ distance $\leq 1^\circ\!.0$. In addition, the concentration of the yield of Čerenkov light in the image “conc” was required, taking account of the energy dependence. Here we have determined above cut parameters as loose as possible to avoid both over-cutting γ-ray events and the distortion of the flatness of the α distribution for background events: by adjusting a cut parameter not to appear any α peak near 0°in the ’on-source’ data removed by the cut, which eventually reduces the systematic errors. The detail is described in T94 .

The resulting event distributions in the combined 1992, 1993 and 1995 data-set are plotted in Fig.1a as a function of α. The α peak appearing around the origin ($\alpha \leq 15^\circ$) in the on-source data are attributed to γ-rays from the Crab, and the number of background events in the α peak region was estimated from the flat region of the α distribution (30°–90°) in the on-source data. Here off-source data was used to verify the non-existence of a peculiar structure of the α plot around the origin without gamma-ray events. The statistical significance of the α peak is calculated using the following: $(N_{\rm on} - \beta \cdot N_{\rm back})/\sqrt{N_{\rm on} + \beta^2 \cdot N_{\rm back}}$, where $N_{\rm on}$ and $N_{\rm back}$ are the numbers of events in the source region ($0^\circ \leq \alpha \leq 15^\circ$) and in the background region ($30^\circ \leq \alpha \leq 90^\circ$) of the on-source data respectively, and β is the ratio of the α range of the source region (15°) to

the background region (60°). The statistical significance of the peak in Fig.1a thus obtained is 7.2σ.

Effects due to the bright star ζ Tau, visual magnitude 3.0, which is located 1.1° from the Crab and within the field of view of the camera, were investigated by the same procedure as used previously (T94). We found no effect which would cause false α peaks.

EDITOR: PLACE FIGURE 1 HERE.

The collecting area as a function of energy and threshold energy of the telescope for gamma-ray showers have been inferred from a Monte Carlo simulation as described in Patterson & Hillas (1990) and T94. In order to obtain the energy spectrum, α plots were made by varying the minimum and maximum numbers of detected Čerenkov photons, required in the event analysis. The energy of gamma-rays is defined as the energy of the maximum flux of simulated gamma-ray events having a similar amount of Čerenkov light to the detected events. The spectrum was then estimated as follows. First, simulated events were generated between 3 TeV and 70 TeV, assuming a differential power law index of −2.6. The collecting area, trigger efficiency and threshold energy corresponding to each α plot were independently estimated from the simulation result, and a spectrum was calculated. Using this new spectrum, the simulation was repeated and the spectrum recalculated. We iterated these steps until the spectral index converged. The resultant differential spectrum, *J(E)*, between 7 TeV and 50 TeV is plotted in Fig.2, and can be written as:

$$J(E) = (2.01 \pm 0.36) \times 10^{-13} (E/7\,\mathrm{TeV})^{-2.53 \pm 0.18}\ \mathrm{TeV}^{-1}\mathrm{cm}^{-2}\mathrm{s}^{-1}, \qquad (1)$$

where the errors are statistical ones only.

The systematic errors on the flux and the index due mainly to the event selection procedure are estimated to be ±30% and ±0.15, respectively. Another systematic error

of 50% on the flux arises from the uncertainty of the absolute gamma-ray energy of 25%, which is due mainly to errors in the estimation of the number of detected photo-electrons and the reflectivity of the telescope mirror. The total systematic error on the flux is 58%.

EDITOR: PLACE FIGURE 2 HERE.

EDITOR: PLACE FIGURE 3 HERE.

The resultant differential spectrum smoothly connects with new results of the Whipple group from 500 GeV and up to 8 TeV (Cater-Lewis et al. 1997) as shown in Fig.2. For comparison with other results above 10 TeV, the integral flux is presented in Fig.3, which is consistent with the result of the Themistocle Group (Djannati-Atai et al. 1995) and several upper limits of gamma-ray flux obtained by array-type experiments (Alexandreas et al. 1991; Amenomori et al. 1992; Karle et al. 1995).

Figs.1b,1c, and 1d show the α plots for the events of $\geq$ 20 TeV, $\geq$ 37 TeV, and $\geq$ 47 TeV, respectively. Note that the α peak above the hadronic background becomes clearer as the threshold energy increases. In order to show the hardness of the observed spectrum, the ratio of the number of gamma rays to that of the background, are plotted as a function of threshold energy of gamma rays in Fig.4, where gamma-rays events in the α peak ($\alpha \leq 15°$) and background events with ($30° \leq \alpha \leq 90°$) were used. These ratios were calculated using the data to which only a simple distance cut were applied in order to avoid an energy dependence of the rejection efficiencies of the imaging cuts for hadrons. The energy dependence of the trigger efficiencies for both gamma rays and hadrons are taken into account using the same Monte Carlo simulation. Fig.4 shows that this ratio increases as the threshold energy rises. This ratio is expected to be sensitive to the existence of the spectral cut-off because the hadron spectrum absolutely extends with the constant index of

–2.7 up to more than hundreds TeV. Assuming the spectral cut-offs of 30, 50 and 100 TeV, the energy dependence of this ratio was simulated including the energy resolution as shown in Fig.4, where both differential indices of ours (–2.53) and the Whipple group (–2.45) were examined. The result obviously favors the nonexistence of the spectral cut-off at least less than 50 TeV: reduced χ^2s of our data are 5.70 (30 TeV cut-off), 2.74 (50 TeV cut-off) and 0.85 (100 TeV cut-off).

In addition, the differential spectrum of the background cosmic rays was calculated from this data to be $(3.2 \pm 0.1) \times 10^{-8} (E/10\,\mathrm{TeV})^{-2.73 \pm 0.03}$ $\mathrm{TeV^{-1} str^{-1} cm^{-2} s^{-1}}$ in the energy range of 13 TeV to 110 TeV, where the error represents only statistical one. It is noted that the differential cosmic ray spectral index can be reconstructed with good accuracy, which also shows the validity of the estimation of the relative energy scale for the gamma rays. The maximum systematic error of our simulation for the cosmic ray flux is $\sim$50% because we assumed all cosmic rays are protons in the simulation. The resultant flux agrees with the recent results of balloon-borne experiments (Ichimura et al. 1993) within $\sim$20% for the proton flux. Thus, the spectra of both gamma rays and cosmic rays are obtained from the same measurement, which is the first attempt as far as we know. It presents the independent and absolute calibration to estimate the energy spectrum in air Čerenkov experiments.

Improvements of the simulation are under way, taking account of the other main ingredients of the cosmic ray flux.

EDITOR: PLACE FIGURE 4 HERE.

4. Discussion

Very high energy gamma rays from the Crab nebula are believed to originate in the shock acceleration of electrons by the pulsar wind in the nebula (Kennel & Coroniti 1984), but a possible origin within the pulsar magnetosphere near the light cylinder (Cheung & Cheng 1994) has not been ruled out, observational proof being lacking. In this region, the strong magnetic field decreases the emissivity of the multi-TeV gamma rays by the electron-positron pair creation process between gamma rays and the magnetic field. Gamma rays above 10 TeV therefore cannot emanate from the vicinity of the light cylinder (Cheung & Cheng 1994). Our observation of gamma rays up to 50 TeV strongly disfavours this idea, and provides direct evidence that the very high energy relativistic particles are accelerated by the pulsar wind.

As mentioned previously, the whole of IC gamma-ray spectrum for the Crab have been calculated by several authors on the basis of the SSC model. Recently it has been pointed out by AA96 that Cosmic Microwave Background (CMB) and infrared (IR) photons emitted from dust in the nebula are the main seed photons for TeV gamma-ray production by the IC process. These effects modify the spectrum of TeV gamma rays from the Crab, causing it to be flatter than that calculated by the simple SSC model. The spectrum above $\sim$ 100 GeV is predicted to steepen as the energy increases, due to the Klein-Nishina limit in the SSC process. On the other hand, the gamma rays produced by IC with low energy seed photons such as CMB or IR are predicted to have flat spectra up to a few TeV (Thomson limit). Consequently, the combined spectrum including the effects of SSC, and IC with CMB and IR, retains its integral index of $\sim$ 1.50 up to the $\sim$ 10 TeV region. Observations of TeV gamma rays by the Whipple, HEGRA,Themistocle, and CANGAROO collaborations are evidence of the significant contribution of IC with CMB and IR.

Furthermore, as the energy increases, the observed spectrum departs from the

theoretical calculations of all models which include only the above contributions such as the calculation of AA96. Intrinsically, the higher energy gamma rays generated by the IC process have a naturally steeper spectrum due to synchrotron energy loss in magnetic fields. Hence all models based on electron processes have difficulty in explaining the observed hard spectrum which extends to beyond 50 TeV.

One simple idea to explain this is to consider the gamma-rays from π° generated by protons which may be included in a pulsar wind and accelerated by its terminated shock similarly to leptons. The spectrum of gamma-rays from π° is expected to retain its hard differential index of ~ -2.1 up to near the maximum accelerated energy. Above $\sim$10 TeV, this component gradually may raise its ratio in the whole gamma-ray spectrum. AA96 presented a calculation based on such an assumption considering proton acceleration in the nebula, in which all parameters, such as the total energy used in proton acceleration, were constrained to satisfy the observational data of the Crab. In the case of protons having an differential index of -2.1, the resulting spectrum of TeV gamma rays keeps its differential index of -2.5 beyond 50 TeV which matches very well with our result. Although it cannot be said that our result is strong evidence of proton acceleration in the Crab nebula, it is supportive of this claim – further observations of the Crab are clearly of great importance.

In order to obtain direct evidence of proton acceleration, two observations are necessary: one is the observation of the extension of the hard spectrum up to 100 TeV, and the other is a measurement of the size of the emission region of gamma rays $\geq$ 10 TeV . In the Crab nebula, very high energy electrons in the multi-TeV region emit both X-rays by synchrotron radiation and TeV gamma rays by IC. The size of the X-ray emission region is therefore directly related to that of the emission region of TeV gamma rays. The *ROSAT* HRI image at 1–2 keV (Hester et al. 1995) suggests the emission region of TeV gamma rays is concentrated within $2'$ of the center of the Crab nebula, if TeV gamma rays are

generated by IC. On the other hand, protons can occupy the cavity within the Crab nebula of diameter $\sim 7'$. If multi TeV gamma rays from the Crab are mainly due to high energy protons, the observed source size would increase as the energy goes above 10 TeV.

T.Tanimori would like to thank F.A. Aharonian for fruitful discussions. This work is supported by a Grant-in-Aid in Scientific Research of the Japan Ministry of Education, Science, Sports and Culture, and also by the Australian Research Council and International Science and Technology Program. T. Tanimori and T.Kifune are grateful for support from the Sumitomo Foundation. The receipt of JSPS Research Fellowships (P.G.E., T.N., M.D.R., K.S., G.J.T. and T. Yoshikoshi) is also acknowledged.

REFERENCES

Aharonian, A. F., et al. 1997, astro-ph/9706019

Alexandreas, D. E., et al. 1991, ApJ, 383, L53

Amenomori, M., et al. 1992, Phys. Rev. Lett., 69, 2468

Atoyan, A. M., & Aharonian, F. A. 1996, MNRAS, 278, 525

Cater-Lewis, D. A, et al. 1997, 25th Int. Cosmic Ray Conf.(Durban), 3, 161

Cheung, W.M., & Cheng, K.S. 1994, ApJS, 90, 827

De Jager, O. C., & Harding, A.K. 1992, ApJ, 396, 161

De Jager, O. C., et al. 1996, ApJ, 457, 253

Djannati-Atai, A. et al. 1995, Proc. 24th Int. Cosmic Ray Conf. (Rome), 1, 315

Goret, P., et al. 1993, A&A, 270, 401

Hara, T., et al. 1993 Nucl. Instr. and Meth., A332, 300

Hester, J.J., et al. 1995, ApJ, 448, 240

Hillas, A.M. 1985, Proc. 19th Int. Cosmic Ray Conf.(La Jolla), 3, 445

Ichimura et al. 1993, Phys. Rev. D, 48, 1949

Kennel, C. F., & Coroniti, F. V. 1984, ApJ, 283, 694

Karle, A., et al. 1995, Astropart. Phys., 4, 1

Nolan, P. L., et al. 1993, ApJ, 409, 697

Patterson, J. R., & Hillas, A.M. 1990, J. Phys. G16, 1271

Patterson, J. R., & Kifune, T. 1992, Australian and New Zealand Physicist, 29, 58

Sommers, P., & Elbert, J. W., 1987, J.Phys. G:Nucl. Phys., 13, 553

Tanimori, T., et al. 1994, ApJ, 429, L61

Vacanti, G., et al. 1991, ApJ, 377, 467

Weekes, T. C., et al. 1989, ApJ, 342, 379

Fig. 1.— (a) The distribution of the image alignment angles relative to the source direction, α, for the final combined data (1992, 1993, and 1995): solid and dashed lines show on- and off-source data, respectively. Also shown are the α distributions of the same data with the threshold energy cuts of (b)$\geq$ 20 TeV, (c)$\geq$ 37 TeV, and (d) $\geq$ 47 TeV, respectively.

Fig. 2.— The differential spectra of the present result in comparison with other experiments: Recent results from the Whipple (Cater-Lewis et al. 1997) and the HEGRA groups (Aharonian et al. 1997). The full line is the power law fit given by equation (1).

Fig. 3.— The integral spectra of the present result in comparison with other experiments. Recent results from the Whipple (Cater-Lewis et al. 1997) and the Themistocle (Djannati-Atai et al. 1995) groups are shown as well as upper limits from the Cygnus (Alexandreas et al. 1991), Tibet (Amenomori et al. 1992), and AIROBICC (Karle et al. 1995). The full line is the power law fit given by $8.4 \times 10^{-13}(E/7\,\mathrm{TeV})^{-1.53}$ cm^{-2}s^{-1}.

Fig. 4.— The ratio of the number of gamma rays to that of background events as a function of threshold energy of gamma rays, where gamma-rays events with $\alpha \leq 15^\circ$ and background events with (30°–90°) were used. Simulated energy dependences of the ratio are also potted, assuming the spectral cut-offs of 30(circle), 50(square) and 100 TeV(triangle). All simulated results are normarized to the observed ratio at 7 TeV. Here both differential indices of ours (–2.53, broken line) and the Whipple group (–2.45, dotted line) were examined.

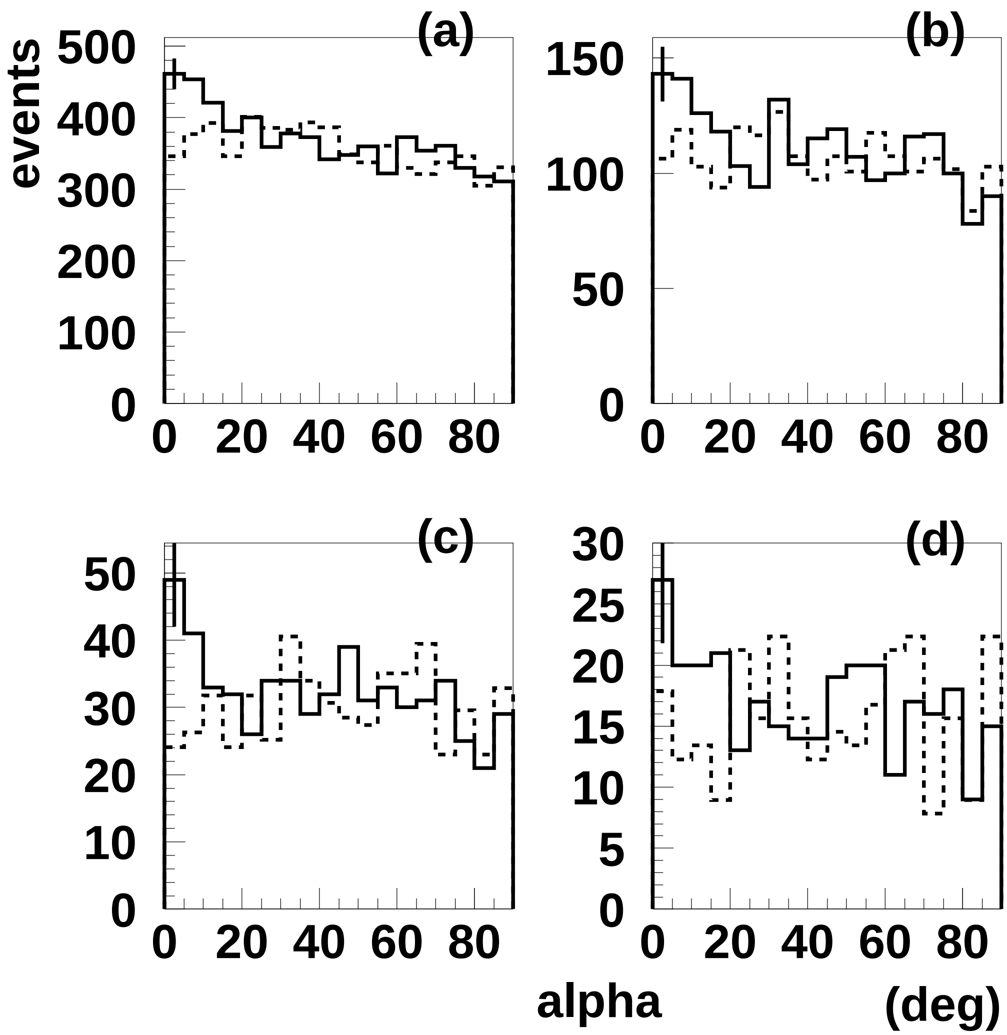

events
alpha
(deg)
(a)
(b)
(c)
(d)
500
400
300
200
100
0
150
100
50
0
50
40
30
20
10
0
30
25
20
15
10
5
0
0 20 40 60 80

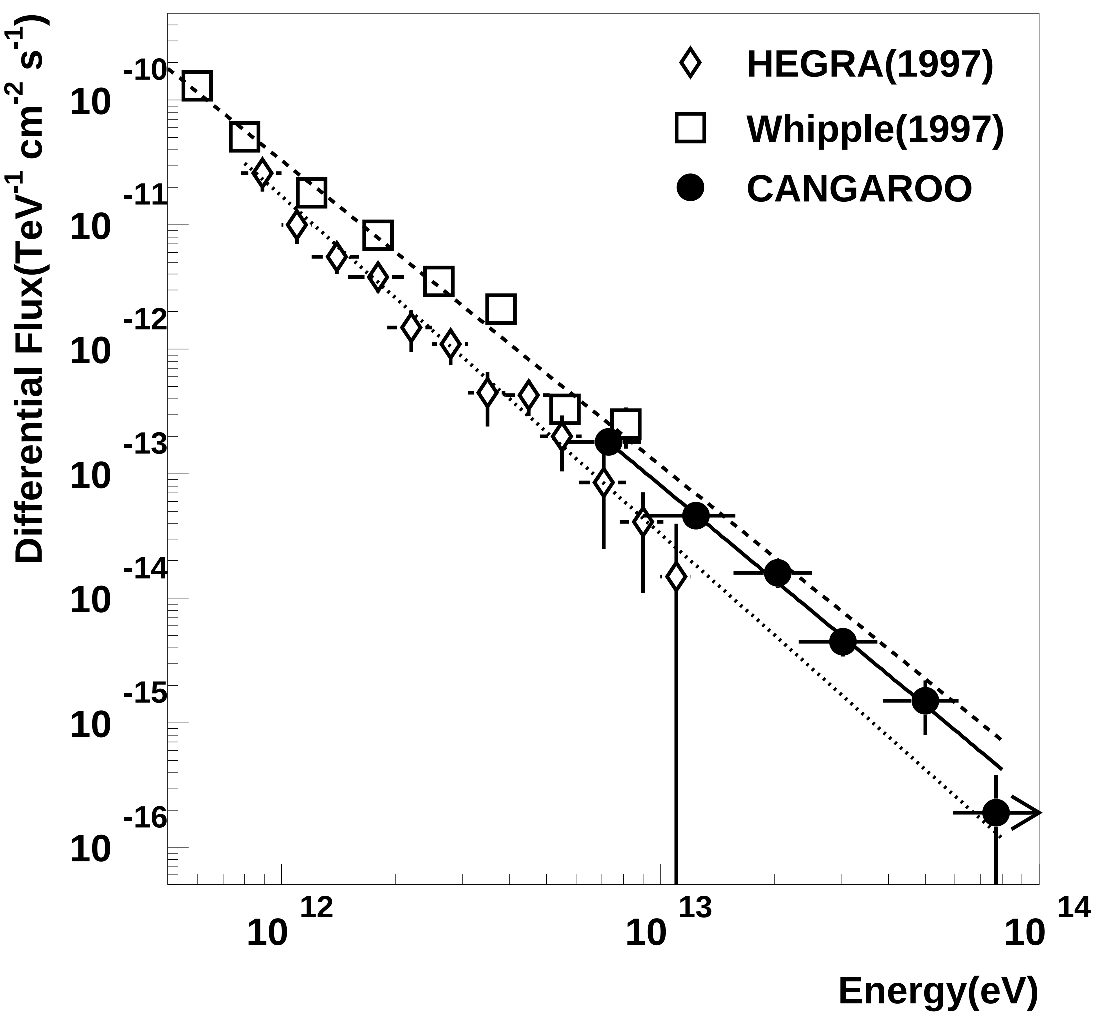
HEGRA(1997)
Whipple(1997)
CANGAROO
Differential Flux(TeV^{-1} cm^{-2} s^{-1})
10^{-10}
10^{-11}
10^{-12}
10^{-13}
10^{-14}
10^{-15}
10^{-16}
10^{12}
10^{13}
10^{14}
Energy(eV)

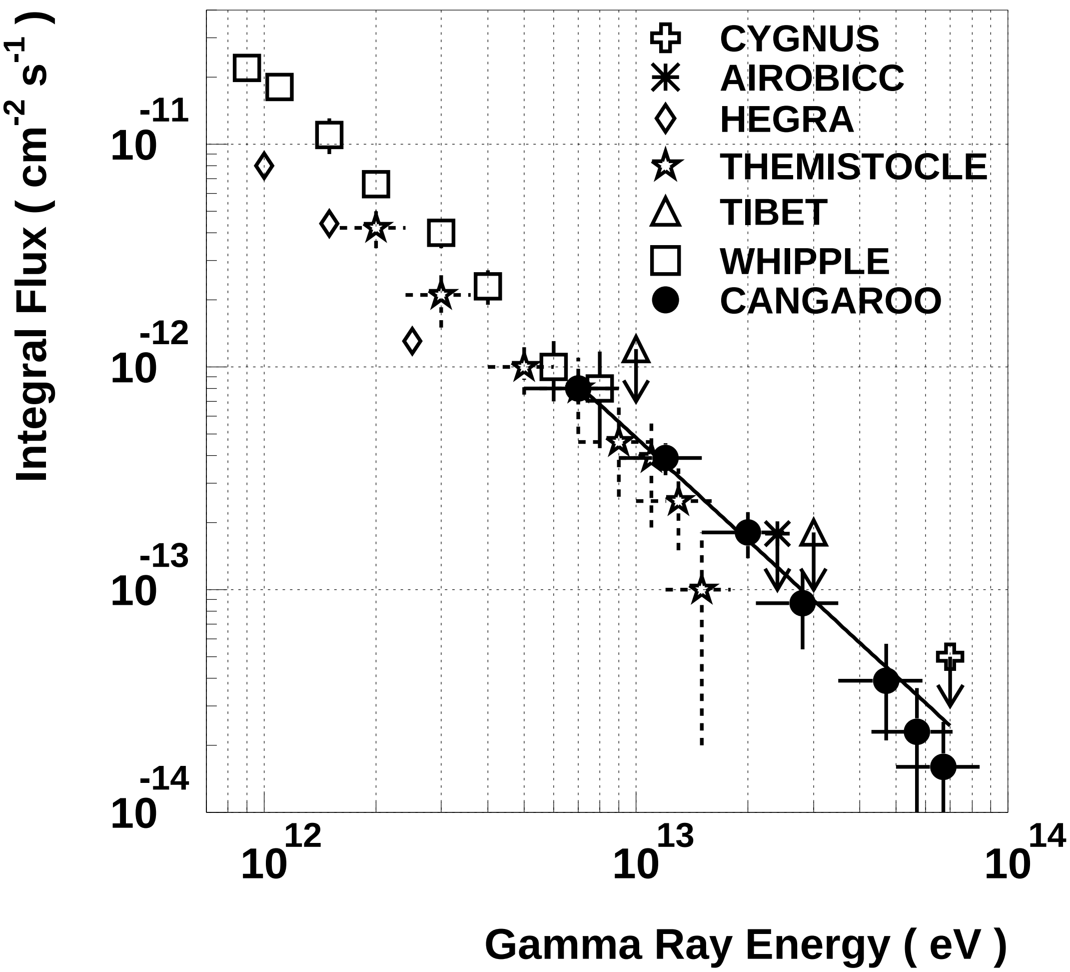
Integral Flux (cm-2 s-1)
10-11
10-12
10-13
10-14
1012
1013
1014
Gamma Ray Energy (eV)
CYGNUS
AIROBICC
HEGRA
THEMISTOCLE
TIBET
WHIPPLE
CANGAROO

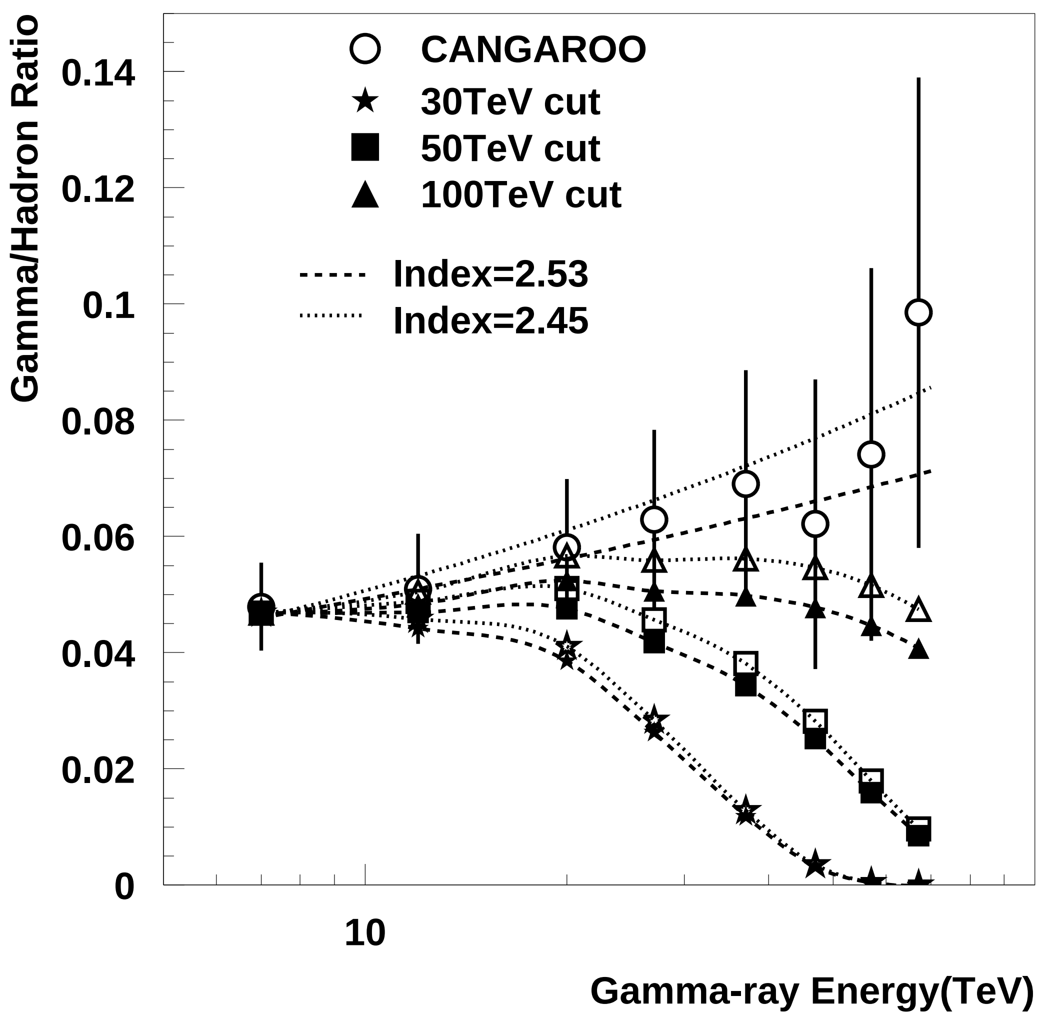

Gamma/Hadron Ratio
0.14
0.12
0.1
0.08
0.06
0.04
0.02
0
10
Gamma-ray Energy(TeV)
CANGAROO
30TeV cut
50TeV cut
100TeV cut
Index=2.53
Index=2.45